Available online at www.sciencedirect.com
SCIENCE DIRECT®
Journal of Power Sources 133 (2004) 135–140
JOURNAL OF POWER SOURCES
www.elsevier.com/locate/jpowsour

Failure mechanism of valve-regulated lead–acid batteries under high-power cycling

J.H. Yan [a,b], W.S. Li [a,*], Q.Y. Zhan [b]

[a] *Department of Chemistry, South China Normal University, Guangzhou, Guangdong 510631, China*
[b] *B.B. Battery Co. Ltd., Raoping, Guangdong 515700, China*

Received 4 August 2003; accepted 27 November 2003

Abstract

A group of valve-regulated lead–acid (VRLA) batteries (12 V, 33 Ah) cycled under high power has exhibited premature failure. The only difference between failed and healthy batteries is the shedding of active material from the positive plates. The dislodged material has been examined by means of X-ray diffraction, scanning electron microscopy, and cyclic voltammetry. It is found that the material has a β-PbO_2 structure. The particles, which are oval in shape with a diameter of about 100 μm, are uniform and well separated from each other. The activity of the material can be restored under pressure. It is concluded that the failure mode of VRLA batteries under high-power cycling is softening of the positive active-material, which eventually results in deterioration of the electrical conductivity and de-activation of the material.

Keywords: Cyclic voltammetry; Failure mechanism; High-power cycling; Lead–acid battery; Positive active-material; Softening

1. Introduction

Lead–acid batteries have been used as a practical power source for over 100 years because of their high performance, low cost, and safety. Great progress has been made since the appearance of the first lead–acid battery. More and more applications of lead–acid batteries will eventuate as the performance is improved further [1].

One of the most promising paths for the lead–acid battery industry lies in valve-regulated lead–acid (VRLA) batteries with deep-cycling capabilities. Over the past few decades, VRLA batteries have been widely used in a number of storage applications, e.g. security systems, emergency lighting, medical equipment, uninterruptible power supplies, automobiles, electrical tools, and electrical vehicles [2]. Other new markets that are emerging for VRLA batteries include aviation, marine, power generation and military applications.

According to the operating regime, VRLA batteries can be classified into two main applications, namely, cycle and standby (float) use. In cycle operation, a battery is deeply discharged until it can no longer release any useful energy. It is then charged and re-used again. When in use, the battery is not connected to a charger. In standby service, by contrast, the battery is continuously charged and functions only when ac power is interrupted.

Recently, a new demand for VRLA batteries has arisen. This is for a power source in which the VRLA batteries co-operate with another power device to function as a new type of power generator. In this system, which is clean and environmentally friendly, the batteries are mounted in a cabinet with a circuit-breaker to safeguard against overcharging, and with a sensor to monitor the temperature. The cabinet is combined with a compact turbine and the entire system serves as a independent energy supply for a community. When the external power demand exceeds the maximum output of the turbine, the batteries automatically start to discharge and supply energy to generator. Conversely, during intervals of low external demand, the turbine charges the batteries. The batteries operate under high-power cycling, i.e. under a service that differs from either normal cycle duty or from standby operation.

Whether or not the application of VRLA batteries is successful depends on their cycle-life. Understanding the failure mechanism of a battery is necessary to prolong this life. Much work has been done in this area [3–11]. The purpose of this paper is to report a failure mode of VRLA batteries under high-power cycling and to determine the failure

* Corresponding author. Tel.: +86-20-85216890; fax: +86-20-85210763.
E-mail address: liwsh@scnu.edu.cn (W.S. Li).

0378-7753/$ – see front matter © 2004 Elsevier B.V. All rights reserved.
doi:10.1016/j.jpowsour.2003.11.075

mechanism by using X-ray diffraction (XRD), scanning electron spectroscopy (SEM), and cyclic voltammetry.

2. Experimental

In a high-power cycle test, 24 batteries (12 V, 33 Ah) were connected in series. The charge–discharge regime is shown in Fig. 1. The cycle is repeated every 2 min to rapidly age the batteries and determine the approximate lifetime under these conditions. The maximum discharge is 60 kW per cycle, and the maximum discharge current reaches 200–250 A in 10 s. After pausing for 50 s, batteries are charged for 20 s. The maximum charging power is 30 kW, so the maximum current during charging exceeds 50 A for all the batteries.

It can be seen from Fig. 1 that batteries are actually run under partial state-of-charge. This duty minimises the passive effect due to high current charging. The batteries are fully charged for 4 h at the cycle charge voltage after every 1000 cycles. Software is used to control the state-of-charge of the batteries to between 70 and 80% during cycling. This is measured by integrating current into and out of the battery over time. The state-of-charge level of the battery is maintained in this range to accommodate the high-power charging pulse. The voltages of the 24 batteries during this cycle are recorded individually. The dc resistance of each battery is calculated from the voltage drop during the discharge pulse.

X-ray diffraction experiments were performed with a D/MAX-3A/Rigaku diffractor with Cu Kα radiation of 30 kV, 30 MA, and $2\theta^\circ$ from 10 to 70° at 12°/min. Scanning electron microscopic studies were performed with a HITACHI S-50 instrument. Cyclic voltammetric experiments were conducted with a PGSTAT-30 system (Autolab, Eco Echemie B.V. company) in a three-electrode cell. The electrolyte was 1.28 g cm^{-3} H_2SO_4 solution. The reference electrode was Hg | Hg_2SO_4 | 1.28 g cm^{-3} H_2SO_4. The counter electrode was platinum with a large area. A microelectrode was used as the working electrode. The electrode was made as follows: a platinum wire with a diameter of 100 μm was sealed in glass and etched to form a cavity, then a powder of positive active-material taken from a battery was pressed into the cavity.

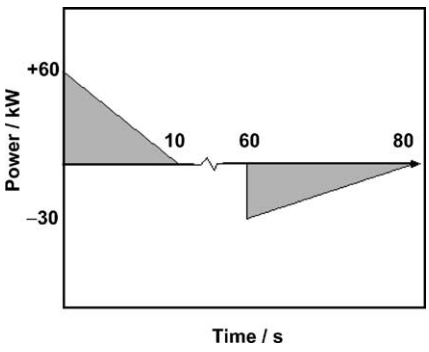

Fig. 1. Regime for high-power cycle test.

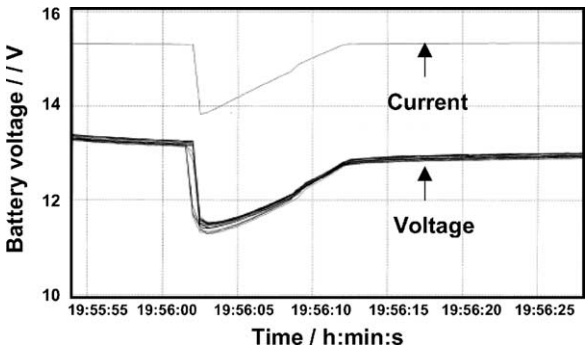

Fig. 2. Normal voltage profile under high-power discharge, first cycle.

3. Results

The change in battery voltage during a discharge pulse is shown in Fig. 2. During the 60 kW discharge, the current typically reaches 200–250 A for a short period. The battery current (although there is no scale) is given by the upper curve in Fig. 2. The voltages of the individual batteries are shown with the scale on the left. The battery voltages are very consistent. This is typical of the performance expected from batteries over a range of state-of-charge from 50 to 100%.

The battery voltage profile during a discharge pulse after 9000 cycles is shown in Fig. 3. It can be seen that the voltage profiles of some batteries deviate from the normal profile. These batteries are showing a high internal resistance. At this point, the battery state-of-charge is between 70 and 80%. Such behaviour is expected, but it is usually due to cell dry-out and normally occurs much later in life. Usually, a high resistance is present regardless of the state-of-charge but, in this case, the high resistance is only present at a reduced state-of-charge.

A separate test was performed to characterise this phenomenon. Discharge pulses were executed at different states-of-charge in intervals that ranged from 100 to 71%. The battery resistance vs. state-of-charge is presented in Fig. 4. The batteries exhibit consistent behaviour and have a low resistance until about 84% state-of-charge, except for one battery that suddenly registers a high resistance. On

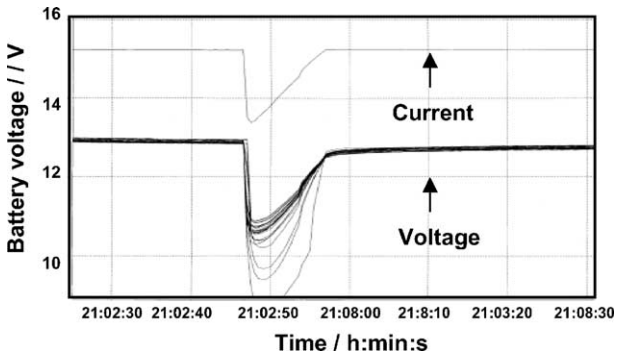

Fig. 3. Voltage profile under high-power discharge, after 9000 cycles.

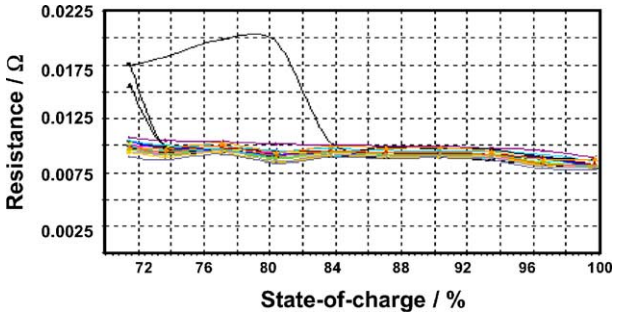

Fig. 4. Battery resistance vs. state-of-charge.

continuing the test, two other batteries display a similar problem. This indicates that this failure is not unique and will eventually occur in all of the batteries in this group.

The battery with high resistance was charged with a small current of 1.65 A (0.05 C) for 24 h, and then rested for another 24 h. At that stage, the open-voltage was 13.08 V. When discharged at the 20 h rate, however, the capacity was only 18 Ah, which was much less than the nominal value of 33 Ah. Clearly, the battery had failed. To understand the failure mechanism, the battery was subjected to an autopsy. The physical state of the positive plates is shown in Fig. 5. It can be seen that the active material has shed from the grid and that the separators are coated with a considerable amount of brown material from the positive plates. No corrosion or deformation of the grids is observed. The negative plates have remained in a healthy condition. Samples of the shed positive active-material were rinsed with de-ionised water, dried, and kept under a dry condition for later experimental uses. For comparison, positive active-material was taken from a good battery after the same number of cycles and from a newly-made battery.

The XRD patterns of positive active-materials from newly-made, cycled (good) and failed batteries are presented

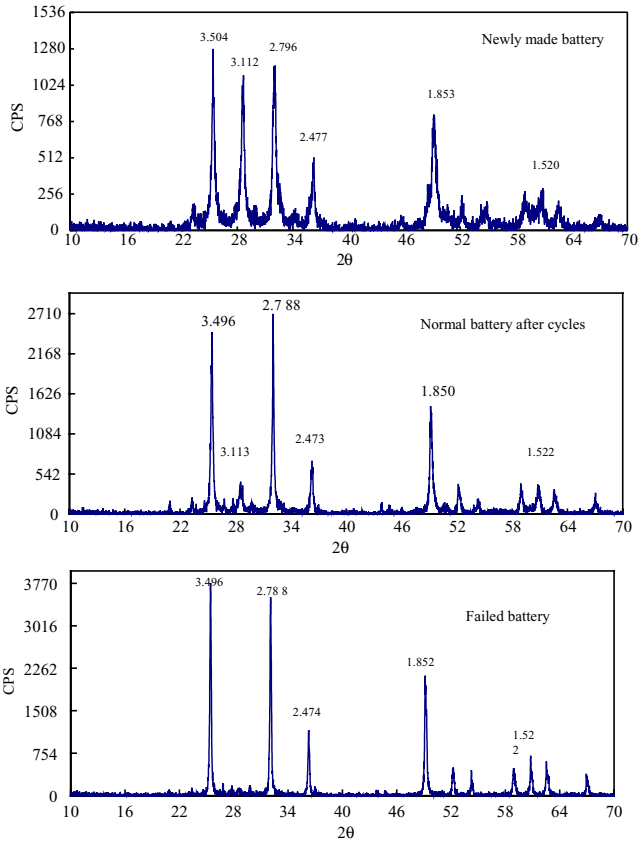

Fig. 6. X-ray diffraction patterns of positive active-materials.

in Fig. 6. The density of the diffraction peaks increases and the width decreases in the order: newly-made battery, cycled (good) battery, failed battery. This indicates that the crystallinity of the active material increases after cycling and that the active materials in the failed battery have the best crystallinity. The XRD of the positive active-material from

Fig. 5. Condition of positive plates from failed battery.

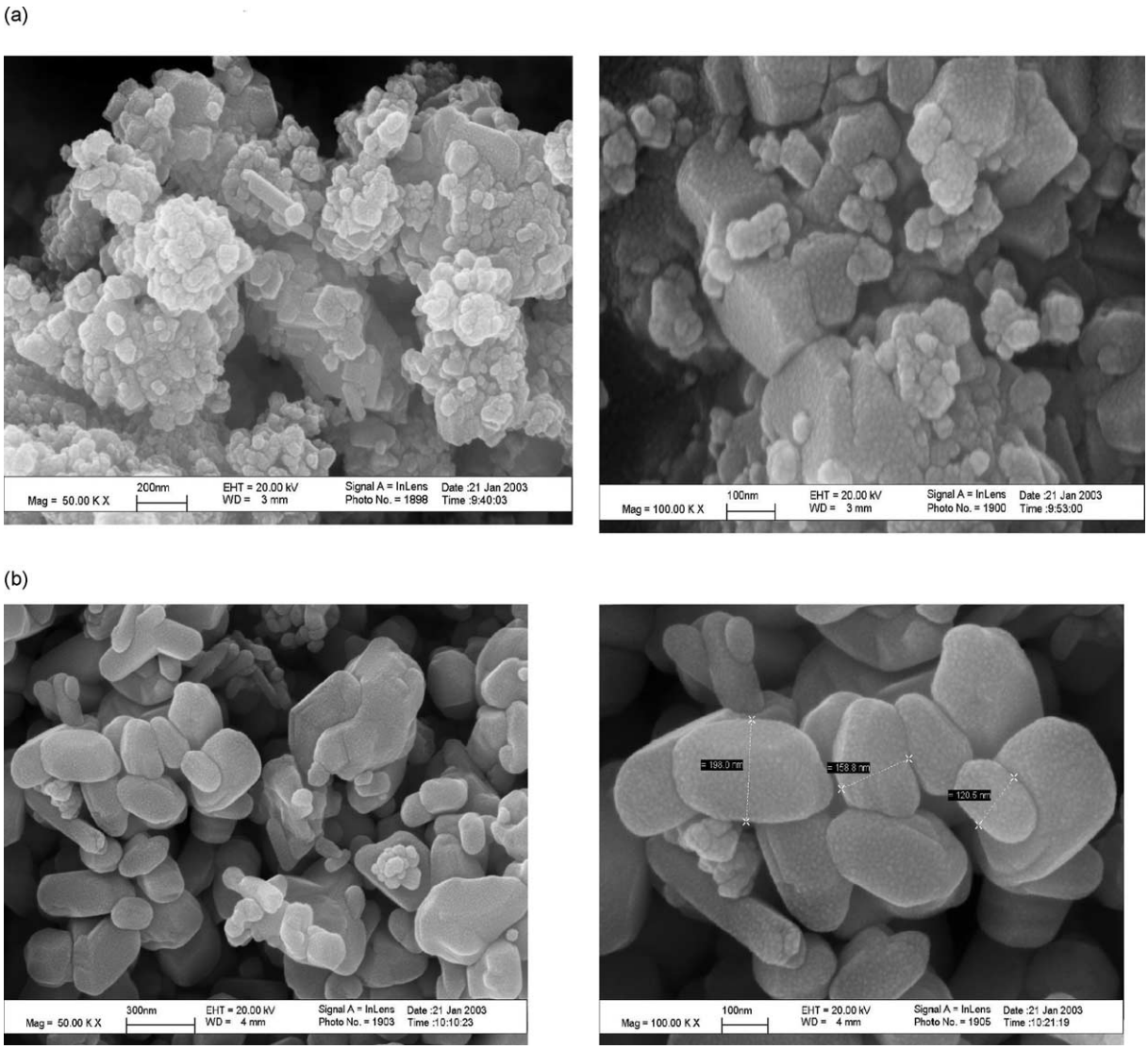

Fig. 7. Crystal morphology of positive active-materials from (a) newly-made and (b) failed battery.

the newly-made battery reveals that the positive material consist of α-PbO_2 and β-PbO_2, characterised at $d = 3.1$ and 3.5 Å, respectively. By contrast, the characteristic peak for α-PbO_2 in the active material becomes weak for the cycled battery, and disappears for the failed battery. The transformation of α-PbO_2 to β-PbO_2 with cycling is quite normal. Rapid formation of β-PbO_2 may lead to premature capacity loss of a battery. The failure of the battery under high-power cycles is related to this rapid formation of β-PbO_2.

The crystal morphology of the positive materials taken from the newly-made and failed batteries is shown in Fig. 7. The crystals from the former battery are arranged in layers and contact each other tightly. On the other hand, the shape and the arrangement of the crystals of the positive active-material from the failed battery are very different. The particles are uniform with an oval shape of a diameter of about 100 μm, and are well separated from each other. Thus, the shedding of positive active-material from the grids in the failed battery is attributed to the formation of β-PbO_2, which has high crystallinity and poor cohesion.

Voltammograms for microelectrodes using positive active-material from newly-made and failed batteries are given in Fig. 8. For the newly-made battery, the reduction peak potential on the first cycle is about −0.1 V more negative than that in the second and the third cycles, and the charge for oxidation and reduction increases after the second cycle. The difference in reduction peak potential between the first and other cycles can be ascribed to the different active materials. Reduction on the first cycle corresponds to a mixture of α-PbO_2 and β-PbO_2, and to β-PbO_2 in later cycles. The increase in charge for oxidation and reduction can be attributed to the good electrical contact in the oxidation and reduction products confined in the cavity of the microelectrode.

For the active materials from the failed battery, the change in the charge passed for oxidation and reduction with cycling

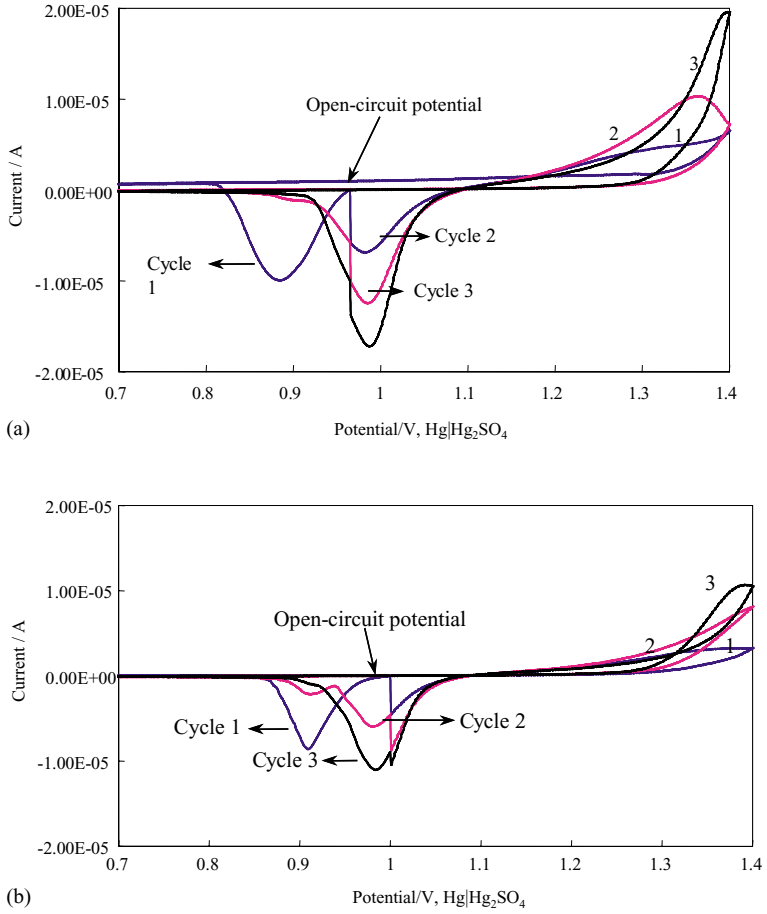

Fig. 8. Cyclic voltammogram for positive active-material microelectrode in 1.280 g cm^{-3} H_2SO_4: (a) newly-made; (b) failed battery.

is similar to that for the active materials from the newly-made battery. Nevertheless, the open-circuit potential of the active materials from the failed battery is more positive than the reduction peak potential in the second and the third cycles, which indicates that the active material behaves like β-PbO_2. The potential of the reduction peak in the first cycle is about 0.07 V more negative than that of the second or third cycle. This can be ascribed to poor electrical contact between the active materials. Apparently, the energy in the active material from the failed battery can be regained by restoring the electrical contact.

4. Discussion

It is known that the failure of VRLA batteries under cycle service may result from softening of positive active-material, short-circuits, deterioration of the absorptive glass-mat separator, and/or plate sulfation. By contrast, failure in float use may result from electrolyte dry-out, thermal runaway, grid corrosion, electrode and busbar ageing, and/or corrosion. Based on the experimental results obtained in this study, the failure of VRLA batteries under high-power cycling is due to the formation of β-PbO_2 with high crystallinity and no cohesiveness. This failure mode leads to softening of the positive active-material.

It has been suggested that charging a lead–acid battery with a larger current can prolong cycle-life [12,13]. This is due to the fact that charging with a larger current favours the formation of small particles of active material that can be recharged effectively. If, however, the charging and discharging currents are too large, the cycle-life of the battery may be impaired. Under such conditions, the small particles of the active material will be separated from each other and, therefore, will be less cohesive. The largest current reaches 250 A in the high-power cycle employed in the present study.

Based on the proposed failure mechanism, some efforts can be made to improve the cycle performance of VRLA batteries under high-power duty. Appropriate oxidation and the particle size of the lead powers used to prepare the positive active-material are important. Lead powders with high oxidation and finer particles are not recommended. Technology that favours the formation of tetrabasic lead sulfate in cured positive plates is beneficial for cycle-life. Curing under high temperature and humidity, together with a low amount of H_2SO_4 in the positive paste, is recommended. Conditions in the formation tank and in the battery that favour the formation of β-PbO_2 are not recommended. With these criteria, the

cycle-life of VRLA batteries cycled under the high-power regime shown in Fig. 1 can be over 30,000 cycles.

5. Conclusions

Valve-regulated lead–acid batteries may experience premature failure when cycled under high power. The failure can be attributed to the rapid formation of β-PbO_2 in the positive active-material. The particles of the material are oval in shape with a diameter of about 100 μm, and are uniform and well separated from each other. The particles are poorly connected, although the electrochemical activity of the material can be regained under pressure.

Acknowledgements

The authors are grateful to Capstone Turbine Corporation, California, USA for assistance with the high-power cycle experiments, and to B.B. Battery Co. Ltd. for financial support to attend the 10th Asian Battery Conference. This project is partly funded by NSFC(20173018) and EYTP of MOE.

References

[1] D. Berndt, Maintenance-Free Batteries, 2nd ed., Research Studies Press, Somerset, UK, 1997, p. 96.
[2] G. Billard, J. Power Sour. 38 (1992) 3–11.
[3] R. Wagner, J. Power Sour. 53 (1995) 153–162.
[4] R.D. Prengaman, in: Proceedings of the Fourth International Lead–Acid Battery Seminar, San Francisco, CA, USA, 1990.
[5] D. Pavlov, A. Dakhouche, T. Rogachev, J. Power Sour. 42 (1993) 71–88.
[6] G.J. May, J. Power Sour. 42 (1993) 147–153.
[7] R.F. Nelson, J. Power Sour. 31 (1990) 3–22.
[8] N.E. Bagshaw, in: T. Keily, B.W. Baxter (Eds.), Power Sources. 12. Research and Development in Non-mechanical Electrical Power Sources, International Power Sources Symposium Committee, Leatherhead, UK, 1989, pp. 113–129.
[9] W.S. Li, Battery Bimonthly (Dianchi) 27 (1997) 172.
[10] R.J. Ball, R. Kurian, R. Evans, R. Stevens, J. Power Sour. 109 (2002) 189–202.
[11] B. Culpin, D.A.J. Rand, J. Power Sour. 36 (1991) 415–438.
[12] Z. Takehara, J. Power Sour. 85 (2000) 29–37.
[13] D. Pavlov, G. Petkova, M. Dimitrov, M. Shiomi, M. Tsubota, J. Power Sour. 87 (2000) 39–56.